REPORT DOCUMENTATION PAGE

Form Approved
OMB NO. 0704-0188

1. AGENCY USE ONLY (Leave Blank)	2. REPORT DATE	3. REPORT TYPE AND DATES COVERED
	January 4, 2001	Final Progress Report - 9/15/97 - 8/14/2000

4. TITLE AND SUBTITLE
Emissivity Engineering Infrared Materials, 3-Dimensionally Patterned by Two Photon Lithography

5. FUNDING NUMBERS
DAAG55-97-1-0384

6. AUTHOR(S)
Bruce Dunn and Eli Yablonovitch

7. PERFORMING ORGANIZATION NAME(S) AND ADDRESS(ES)
University of California, Los Angeles;
Department of Materials Science and Engineering 6532 Boelter Hall;
Los Angeles, CA 90095-1595

8. PERFORMING ORGANIZATION REPORT NUMBER

9. SPONSORING / MONITORING AGENCY NAME(S) AND ADDRESS(ES)
U. S. Army Research Office
P.O. Box 12211
Research Triangle Park, NC 27709-2211

10. SPONSORING / MONITORING AGENCY REPORT NUMBER
ARO 37664.6-PH

11. SUPPLEMENTARY NOTES
The views, opinions and/or findings contained in this report are those of the author(s) and should not be construed as an official Department of the Army position, policy or decision, unless so designated by other documentation.

12 a. DISTRIBUTION / AVAILABILITY STATEMENT
Approved for public release; distribution unlimited.

12 b. DISTRIBUTION CODE

13. ABSTRACT (Maximum 200 words)

The objective of this program is to make infrared pigments whose emissivity can be controlled. The principal approach we have taken is to make 3-dimensionally microstructured metallo-dielectric materials by two-photon lithography in photoresist, and back-filling with metals. In this program we demonstrated that we can quickly and efficiently fabricate 3-d microstructures in photoresist using a diode pumped Ti-sapphire mode-locked laser in combination with a mechanical scanning technology. Metal back-filling of copper into porous membranes was accomplished using electrodeposition methods and complementary fundamental studies were able to establish some of the details of this metallization process. Initial results using self-assembly methods for metallization were also obtained. Another approach for producing 3-d metallo-dielectric structures, based on the direct writing of silver structures by two-photon processes, was also demonstrated. In addition to experimental work, this program included computational activities. An analysis of the resolution limits of two-photon lithography showed that a doubling of resolution was possible. Other studies in this program included the design of frequency selective grid structures and an analysis showing that 1-d interference filters can be used to achieve a broad reflection spectrum.

14. SUBJECT TERMS	15. NUMBER OF PAGES
Two-photon lithography, metallo-dielectric structures, electrodeposition, infrared pigments	41
	16. PRICE CODE

17. SECURITY CLASSIFICATION OF REPORT	18. SECURITY CLASSIFICATION ON THIS PAGE	19. SECURITY CLASSIFICATION OF ABSTRACT	20. LIMITATION OF ABSTRACT
UNCLASSIFIED	UNCLASSIFIED	UNCLASSIFIED	UL

NSN 7540-01-280-5500

Standard Form 298 (Rev.2-89)
Prescribed by ANSI Std. 239-18
298-102

Enclosure 1

MASTER COPY: PLEASE KEEP THIS "MEMORANDUM OF TRANSMITTAL" BLANK FOR REPRODUCTION PURPOSES. WHEN REPORTS ARE GENERATED UNDER THE ARO SPONSORSHIP, FORWARD A COMPLETED COPY OF THIS FORM WITH EACH REPORT SHIPMENT TO THE ARO. THIS WILL ASSURE PROPER IDENTIFICATION. NOT TO BE USED FOR INTERIM PROGRESS REPORTS; SEE PAGE 2 FOR INTERIM PROGRESS REPORT INSTRUCTIONS.

MEMORANDUM OF TRANSMITTAL

U.S. Army Research Office
ATTN: AMSRL-RO-BI (TR)
P.O. Box 12211
Research Triangle Park, NC 27709-2211

☐ Reprint (Orig + 2 copies)
☐ Technical Report (Orig + 2 copies)
☐ Manuscript (1 copy)
☒ Final Progress Report (Orig + 2 copies)
☐ Related Materials, Abstracts, Theses (1 copy)

CONTRACT/GRANT NUMBER: DAAG55-97-1-0384

REPORT TITLE: Emissivity Engineering Infrared Materials, 3-Dimensionally Patterned by Two Photon Lithography

is forwarded for your information.

SUBMITTED FOR PUBLICATION TO (applicable only if report is manuscript):

Sincerely,

Bruce Dunn
Professor

Enclosure 3

Emissivity Engineered Infrared Materials, 3-Dimensionally Patterned by Two Photon Lithography

Final Progress Report

Bruce Dunn and Eli Yablonovitch

Period Covered: 9/15/97 – 8/14/2000

U.S. Army Research Office

DAAG55-97-1-0384

University of California, Los Angeles

TABLE OF CONTENTS

3) List of Appendixes, Illustrations and Tables

Appendix I.

"Highly Controlled Dielectric Emissivity (HIDE)"
(Subcontractor report submitted by Rockwell Science Center)

4) Statement of the problem studied

The problem studied this program involved the use of two-photon lithography to create artificial microstructures for infrared emissivity engineering. In effect, we sought to develop a "laser printer" for 3-dimensional structures, including photonic crystal structures. To complement this new type of printer, we studied and developed infrared pigments, the writing media and materials processing protocols needed for applications with controlled infrared emissivity. The principal approach we have taken is to make 3-dimensionally microstructured metallo-dielectric materials by 2-photon lithography in photoresist, and back-filling with metals. An alternative approach has involved the direct writing of metal structures by two-photon processes. The computational studies associated with this program have included an analysis of two-photon lithography resolution, frequency selective grid structures and the use of interference filters to achieve a broad reflection spectrum.

5) Summary of the most important results

a) Construction of Two-Photon 3-d Laser Printer

We demonstrated that we can quickly and efficiently fabricate 3-d microstructures in photoresist using our diode pumped Ti-sapphire mode-locked laser and a mechanical scanning technology used for "mastering" of CD-ROM's. We formed a "lincoln log" lattice in which one layer consists of 2 μm thick "logs" laid horizontally, while in the next layer the "logs" are laid vertically. The pattern then repeats. All of our experiments used the photoresist SU-8. Enabling experiments with SU-8 had shown that single-shot, two-photon exposures allowed 3-d polymer structures to be fabricated at MHz repetition rates.[1] In fabricating the 3-d microstructure we scanned the 1 μm focus of our Ti:Sapphire laser (outputting 50 femtosecond pulses at 100 MHz) at nearly 100 mph in the 50 μm layer of photoresist, all the while controlling the focus position to within a fraction of a micron. We also investigated using laser pulses in parallel to increase the writing speed to about 1 cm^2/s. In a related effort, we studied the resolution enhancement that two-photon absorption provides. By using multiple adjacent frequencies to pump the two photon absorption, a doubling of the spatial resolution becomes possible.

b) 3-d Metallo-Dielectric Structures by Metal Backfilling

This activity was carried out by the Rockwell Science Center. In summary, four different methodologies were examined. Most of the research emphasized electrodeposition methods, however, self-assembly approaches were also investigated. The electrodeposition studies demonstrated the general robustness of this approach for the back filling of copper into microporous membranes. A number of studies were carried out in an attempt to understand how the metallization may be sustained deeper into the microstructures or in very fine microstructures; the electrochemical process for attaining microstructures was found to have complex dynamics. The deposition nucleates along the microstructure, but the deposition was difficult to contain within the two-dimensional structure because of the dendritic growth of the deposit. Self-assembly methods offer an alternative approach for fabricating 3-d metallo-dielectric structures. Appropriate recipes were developed for materials preparation of ordered, dielectric microstructures with metallization by dissociation of metal salts. A full description of the different methods investigated in this part of the program is contained in Appendix I.

c) Direct Writing of Metal Structures

We have demonstrated a photographic-like approach for producing three-dimensional silver structures.[2] The photographic medium consists of a liquid phase immobilized in the pores of a SiO_2 matrix prepared by the sol-gel process. Different silver salt solutions comprise the liquid phase; these solutions were chosen on their ability to either form a stable latent image or to precipitate silver as required in the development process. Fabrication is based on the formation of a latent image defined by laser irradiation. Multiphoton processes are involved in image formation, allowing features to be written directly into the interior of the matrix in a single fabrication step. After laser exposure, the wet gels are solvent exchanged with a second Ag salt as the development of the image is accomplished from the controlled reduction of a $AgClO_4$ solution. A number of different 3-d silver structures have been written including spirals with diameters greater than 1 mm. The ability to directly write three-dimensional metallic objects in a medium that is based on sol-gel processing is expected to generate new opportunities for metallodielectric structures.

d) Two-Photon Photographic Processes

Early in the program, we investigated two-photon absorption in commercial photographic film and paper.[3] At that time we thought that this material could be an interesting writing medium for the two-photon, 3-d laser printer. In our experiments, a high-intensity laser pulse exposure led to image formation in commercial photographic media at wavelengths and fluences at which one-photon processes could not produce images and well below the optical damage thresholds of the media. This work represents the first demonstration of the visual recording of images produced by a two-photon (or multiphoton) process. By using an appropriate medium, multiphoton photography affords an opportunity for 3-d image storage.

e) Computational and Theoretical Studies

Two-photon lithography is in its infancy, and relatively few papers have been published in this area. In the first few months of the program we carried out a fundamental analysis of the resolution limits of two-photon lithography.[4] We found that ordinary two-photon lithography showed only an apparent improvement of resolution, but it came at the expense of tighter process and exposure control. By using multiple adjacent frequencies to pump the two-photon absorption, a true doubling of the spatial resolution becomes possible. We believe this idea has implications for high resolution lithography and, accordingly, we have filed for a U.S. patent.[5]

We also carried out two other computational activities. In one case, we showed how 1-d layered interference filters can be used to achieve a broad reflection spectrum.[6] Our approach is to start with the least index contrast that produces the narrowest omni-directional spectral reflector, and then gradually vary the inter-layer spacing down through the successive layers, i.e. chirp the layer period. In this way an arbitrarily wide spectral range can be covered with only a modest index contrast provided that the average refractive index is > 2. Another computational activity has involved the design of frequency selective wire grids. We have developed a useful computational capability to analyze various shapes of wire grid structures. This is a computer program based on the application of an integral equation with periodic structure boundary conditions.

6) Listing of publications

a) Papers published in peer-reviewed journals

G. Witzgall, R. Vrijen, E. Yablonovitch, V. Doan, and B. Schwartz, "Single-shot two-photon exposure of commercial photoresist for the production of three-dimensional structures," *Opt. Lett.* **23**, 1745 (1998).

E. Yablonovitch, Engineered omnidirectional external-reflectivity spectra from one-dimensional layered interference filters. *Opt. Lett.* **23**, 1648 (1998).

E. Yablonovitch and R. Vrijen, "Optical projection lithography at half the Rayleigh resolution limit by two-photon exposure," *Opt. Eng.* **38**, 334 (1999).

P.-W. Wu, B. Dunn, E. Yablonovitch, V. Doan, and B. J. Schwartz, "Two-photon exposure of photographic film," *J. Opt. Soc. Am. B* **16**, 605 (1999)

P.-W. Wu, W. Cheng, I. Martini, B. Dunn, B. J. Schwartz and E. Yablonovitch, "Two-Photon Photographic Production of Three-Dimensional Metallic Structures within a Dielectric Matrix," *Adv. Mater.* **12**, 1438 (2000).

c) Papers presented at meetings, but not published in conference proceedings

B. J. Schwartz, V. Doan, B. Dunn, P.-W. Wu, El Yablonovitch, G. Witzgall and R. Vrijen, "Direct Fabrication of Three-Dimensional Structures by Two-Photon Lithography", Materials Research Society, Boston, MA, November, 1999 (Invited talk).

P-W. Wu, B. Dunn, V. Doan, B.J. Schwartz, E. Yablonovitch and M. Yamane, "Controlling the Spontaneous Precipitation of Silver Nanoparticles in Sol-Gel Materials", 10th International Workshop on Glasses and Ceramics from Gels, Yokohama, Japan, September, 1999.

d) Manuscripts submitted, but not published

P.-W. Wu, B. Dunn, V. Doan, B. J. Schwartz, E. Yablonovitch, and M. Yamane, "Controlling the Spontaneous Precipitation of Silver Nanoparticles in Sol-Gel Materials", *J. Sol-Gel Sci. and Technol.* Accepted for publication; to be published in 2001.

7) Participating scientific personnel:

UCLA:
Professors: Bruce Dunn, Eli Yablonovitch, Yahya Rahmat-Samii, Benjamin J. Schwartz, Oscar Stafsudd
Post-Doctoral: Rutger Vrijien, Kang-Wook Kim, Dmitriy Korobkin, Ignacio Martini
Graduate students receiving advanced degrees while employed on this project:
Vinh Doan (M.S., 1999), Yanlin Wu (M.S. 1998), Pu-Wei Wu (Ph.D. 1999)
Other Graduate Student Contributors:
George Witzgall, Ivan Alvarado, Joel DiCecco, Thomas Jun, Alon Barlevy
Rockwell Science Center:
Martin Kendig, Sam Jeanjaquet, Haluk Sankur, Young Chung, Monte Khoshnevisan

8) Report of Inventions:
Patent application: "Ultra-High Resolution Multi-Photon Lithography"

9) Bibliography

1. G. Witzgall, R. Vrijen, E. Yablonovitch, V. Doan, and B. Schwartz, "Single-shot two-photon exposure of commercial photoresist for the production of three-dimensional structures," *Opt. Lett.* **23**, 1745 (1998).
2. P.-W. Wu, W. Cheng, I. Martini, B. Dunn, B. J. Schwartz and E. Yablonovitch, "Two-Photon Photographic Production of Three-Dimensional Metallic Structures within a Dielectric Matrix," *Adv. Mater.* **12**, 1438 (2000).
3. P.-W. Wu, B. Dunn, E. Yablonovitch, V. Doan, and B. J. Schwartz, "Two-photon exposure of photographic film," *J. Opt. Soc. Am. B* **16**, 605 (1999)
4. E. Yablonovitch and R. Vrijen, "Optical projection lithography at half the Rayleigh resolution limit by two-photon exposure," *Opt. Eng.* **38**, 334 (1999).
5. E. Yablonovitch, "Ultra-High Resolution Multi-Photon Lithography", UC Case No. CA 98-047-01, filed, December, 1997.
6. E. Yablonovitch, Engineered omnidirectional external-reflectivity spectra from one-dimensional layered interference filters. *Opt. Lett.* **23**, 1648 (1998).

APPENDIX I.

HIGHLY CONTROLLED DIELECTRIC EMISSIVITY (HIDE)

Subcontractor Report Submitted by Rockwell Science Center

Highly Controlled Dielectric Emissivity (HIDE)

Submitted by:
Rockwell Science Center
1049 Camino Dos Rios
Thousand Oaks, CA 91360

Subcontract to UCLA
Subcontract No. 0190 G 9B005

Prime Contract No. DAAG55-97-1-0384

Period of Performance: August 03, 1998 through August 14, 2000

November 2000

RSC Principal Investigator: Dr. Martin Kendig

RSC Program Manager: Dr. Monte Khoshnevisan

Highly Controlled Dielectric Emissivity (HIDE) Materials

Rockwell Science Center Effort as Subcontractor to UCLA

1.0 Executive Summary (Rockwell Science Center Effort)

This Rockwell Science Center (RSC) effort was under the "Highly Controlled Dielectric Emissivity (HIDE)" program for UCLA, the prime contractor to DARPA/Army (Prime Contract Number DAAG55-97-1-0384). The subcontract to RSC (Subcontract No. 0190 G 9B005, internal RSC number G.O. 73114) was primarily aimed at developing methods to backfill dielectric microstructures with metals, in order to control their reflectance and emissivity over a wide spectral range of electromagnetic spectrum. The twenty-seven month RSC studies explored a number of approaches that showed promise for finely controlled metallization applications, with potential for future scale-up to large area coverage at affordable cost. Much was learned about the metallization process, particularly by an electrochemical method, which was used to metallize through micro-pores. We evaluated the electrochemical process in terms of its potential for back-filling dielectric structures, and uncovered process complexities for applications to ultra-fine structures for future photonic crystals in the infrared or shorter wavelengths, to control emissivity. The findings can prove useful for metal backfilling of fine dielectric structures and photonic crystals for the microwave or infrared. Using these techniques, complete 3-dimensional metallic photonic crystals can be created starting with the corresponding dielectric templates that may be totally removed after metallization. The properties of dielectric photonic crystals may also be altered by addition of partial metal microstructures as well (i.e., hybrid metal & dielectric) using electrochemical methods similar to those developed here.

This work demonstrates the general robustness of electrochemical back filling of micro-porous membranes. Electrodeposited Cu from acid copper baths and copper pyrophosphate baths tend to nucleate from an evaporated Au cathode base along the walls of the porous structure. While this poses no problems for electrodeposition in 1 μm structures, direct current electrodeposition in larger structures results in the formation of hollow structures. However, the

tendency for the deposition of hollow structures in the larger pores (10 μm vs 1 μm) can be overcome, at least in the case of acid copper and copper pyrophosphate, through deposition under conditions of controlled applied cyclic potential.

The electrochemical process for microstructures was found to have complex dynamics and is not yet fully understood. During the course of this effort, we explored some fundamentals of the process, in an attempt to understand how the metallization may be sustained deeper into the microstructures, or in very fine microstructures. Special cells were fabricated using micro-optical fabrication process for a portion of this study and tests were carried out; it was leaned that dendrite growth will interfere with such two-dimensional studies of the deposition process, and more in-depth studies would be required.

A small level of RSC effort near the end of the program was directed at examination of an interesting method to create photonic crystals, including the metallization, through a self-assembly process. This technique turned out to offer significant promise, even though the program resources allowed only the development of partially ordered structures. The method will be pursued further as a part of other programs, targeting applications of photonic crystals that go beyond emissivity control, such as agile beam steering, filtering, waveguides, or wavelength division multiplexing (WDM) applications. The method is obviously applicable to emissivity control as well.

In summary, the results of the overall studies in this program have contributed to methodologies that will allow fabrication of photonic crystals or micro-porous structures with various fractional metal content, from all-dielectric, to fully metallic. These include: 1) metal matrix electrodeposited onto dielectric microstructures (for example, two-photon lithographically produced starting materials), 2) electrodeposited metal matrix around air micro-pores (after removal of the dielectric material), 3) metal matrix deposited on polymer microspheres by a chemical dissociation process from metal salt solution, or 4) metallic lattice deposited by dissociation, surrounding micro air-spheres. The methods could be important for a number of future applications of photonic crystals by advancing the state of the art and providing process tools to engineer such materials. Many applications are likely to emerge for photonic crystals in

the infrared and shorter wavelengths in the next few years, including numerous DoD laser and photonic systems, in addition to emissivity control, and a myriad of commercial applications. Some of these applications will be pursued by RSC, independently, or in collaboration with UCLA. For example, a new DARPA/MTO program [1], involving RSC and UCLA will explore the super-prism properties of photonic crystals for agile beam steering, where the methods explored in this program are expected to provide some of the required technology and understanding.

2.0 Electrochemical Backfilling Studies

2.1 Background

An approach for constructing of highly controlled dielectric emissivity materials involves electrolytic back filling of a three dimensional porous matrix in a dielectric material. A conceptual diagram of the general approach is shown in Fig. 1, with the different steps labeled sequentially. Accordingly, a metallic substrate (1) is coated with a photo-polymer (2), that is photo-sensitized image-wise in three dimensions (3). These three steps have been demonstrated on a small structure at UCLA. The resulting specimen could then be coated with electroless copper, or evaporated copper or gold followed by electrodeposition of a supportive metal backing (4). The specimen will then be exposed to a developer (alkaline) that releases the highly structured, porous dielectric film which is metal-backed (5). The film will then be back-filled by electrodeposition (6) to form the HIDE material (7). Depending on the desired structure for the photonic crystal, the dielectric structure may be allowed to remain under the metal overcoat, or dissolved away by appropriate chemical treatment.

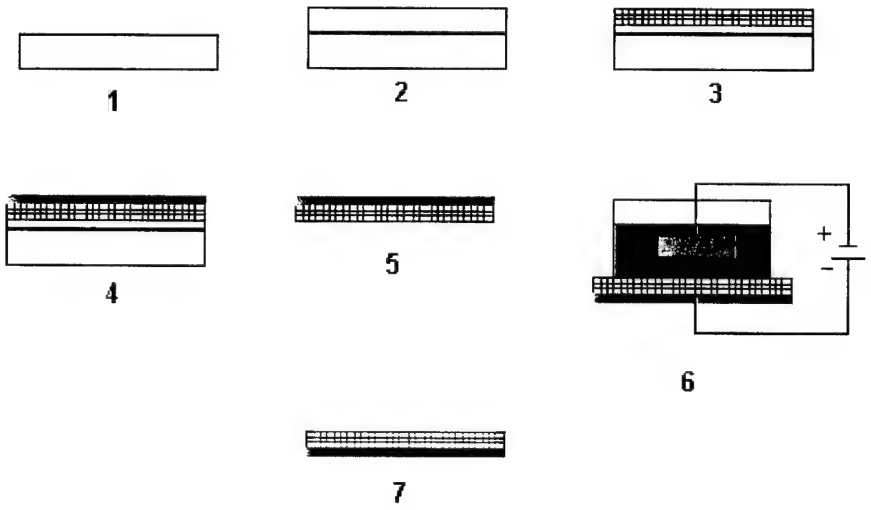

Fig. 1. Conceptual steps in development of metallic photonic crystals. Metallic substrate (1); coated with photo-polymer (2); photo-polymer three-dimensionally photo-sensitized (3); thin metal coat, and electro-deposited metal backing (4); released porous dielectric film metal-backing (5); back-filling by electro-deposition (6); resulting HIDE material (7).

The RSC task focused on defining the process necessary for back-filling porous dielectric structures with metal. The approach taken involved electro-deposition of Cu within a three-dimensional porous dielectric. In order to demonstrate the electro-deposition approach and to identify process parameters necessary to form the deposits, model micro-porous dielectric membranes have been used to test the concept of backfilling by electrochemical deposition.

2.2 Electro-deposition Approach

2.2.1 General Considerations

In order to demonstrate electrochemical backfilling of porous dielectric structures, we carried out experiments to deposit Cu from a Cu pyrophosphate bath in the highly uniform pores of a Poretics® polycarbonate track etch filter. This filter material was selected to serve as an example of a fine micro-structure, in preparation for other, more finely structured materials representative of photonic crystals designed for HIDE applications in the infrared. The objective here was to establish the science of metal backfilling of fine 3-D structures, for future applications to more realistic HIDE materials, which are now more research items and are not widely available.

Although successful deposition occurs if Cu nucleates in the pores of microstructures, the nucleation does not always occur. Rather, Cu deposits between the filter and a backing electrode. It is not entirely clear what controls the nucleation in the pores. Lack of nucleation in the pores will most likely not be a problem in the process described in Fig. 1, since the contact between the backing electrode and the porous structure will leave no gap for the parasitic deposition. Hence, nucleating in the pores of a detached filter did not seem to be the primary problem to be solved for this program. The more important challenge was to obtain uniform (fully-dense) deposition within the porous structure.

2.2.2 Experimental Details

Plating Solutions

Two generic copper plating baths were investigated, the copper pyrophosphate bath and acid copper. The copper pyrophosphate plating bath has the following composition:

- 151 g/L $K_4P_2O_7$
- 52.5 g/L $CuP_2O_7 \bullet x\ H_2O$
- pH adjusted to 8 with H_3PO_4

This bath was prelectrolyzed with two Cu plate electrodes biased at 0.7 V for 16 h. This process electrochemically sweeps out any contaminants onto the cathode and oxidizes organic contaminants on the anode. In some instances the solution also contained 30 μM/L of 2,5-dimercapto-1,3,4-thiadiazole and was prelectrolyzed with Cu plates at 5-10mAcm^2 for 16 h aged at 45-60 degrees C overnight in order to assure the equilibrium formation of the dimeric complex [2].

The acid Cu bath was prepared from the LeaRonal High Throw Acid Copper bath, having the following composition:

- Purified liquid $CuSO_4$ 147.5ml/l
- Concentrated H_2SO_4 180 ml/l
- Concentrated HCl 0.16ml/l
- DI Water Balance

The bath was carbon treated with 9g/l granular carbon and filtered. No leveler or grain refiners were added.

Plating Configurations

Copper was electro-deposited from a Cu pyrophosphate bath, using different electrochemical cell configurations of micro-porous filters (Poretics® polycarbonate track etch (PCTE) membrane filters or Poretics polyester membrane filters) coated with evaporated Au. Specifically, we have considered the following configuration (shown schematically in Fig. 2A and 2B.) These respective configurations can be denoted in the following way:

(1) NC/PS/Au/CuP (Fig. 2A.)

(2) NC/Au/PS/CuP (Fig. 2B.)

where

NC = non-conducting substrate (glass)

Au: evaporated gold cathode (applied to the porous filter)

PS: Porous Sample (filter)

CuP: Copper Pyrophosphate bath

CuPL: Copper Pyrophosphate with leveling agent

CuPLT: Copper Pyrophosphate with Leveling agent and plated at 50^{o} C Temperature

ACu: Acid Copper electrolyte

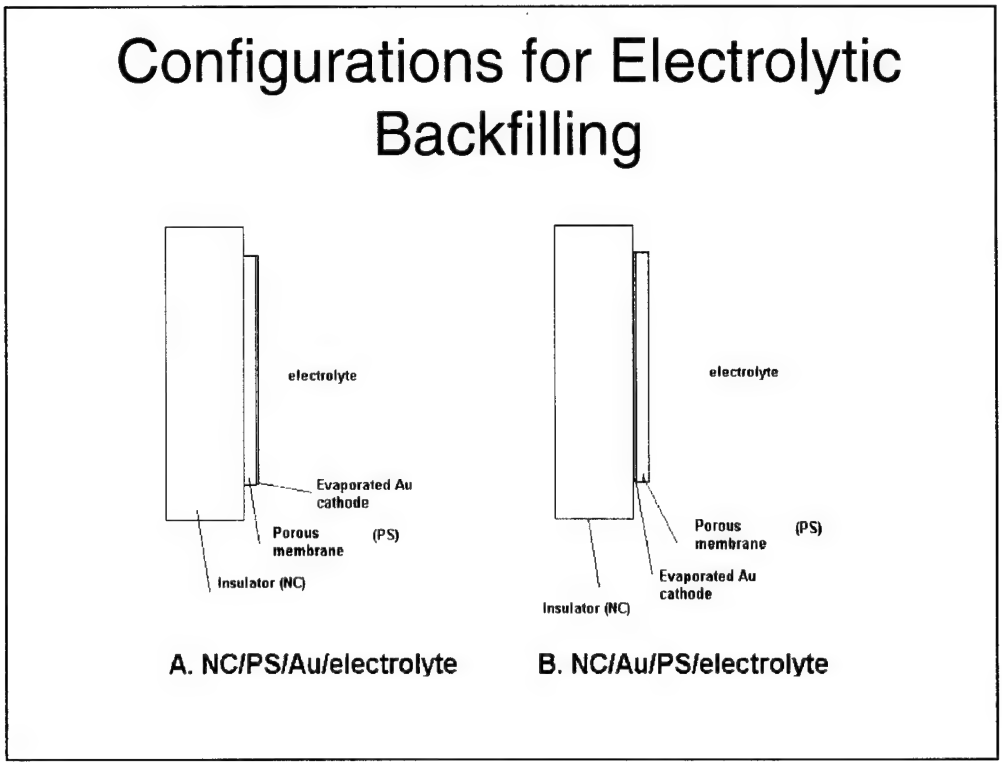

Fig. 2. Configurations for electrolytic backfilling (see text for definition of terms).

The electrochemical cell developed for microstructure metal backfilling uses a gasket sealed glass cylinder, and contains a superficial filter surface area of 8.3 cm^2 and is shown schematically in Fig. 3. It contains a Cu wire anode (counter electrode) and saturated calomel (SCE) reference electrode. The porous media membranes are sealed using a rubber gasket.

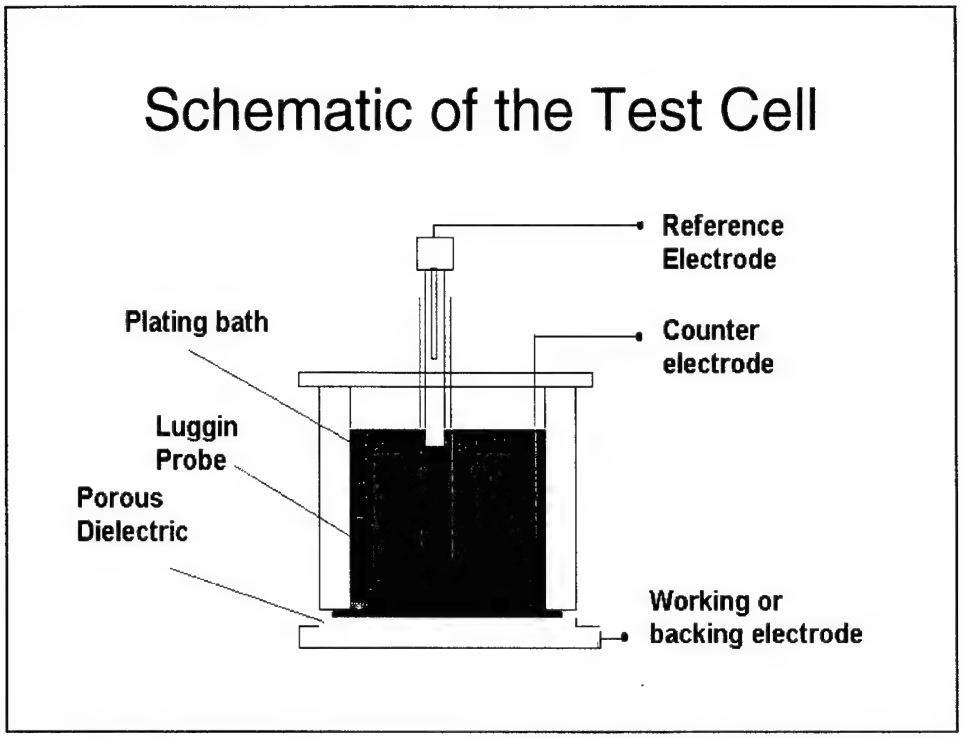

Fig. 3. Schematic diagram of the electro-deposition Test Cell.

Plating Methods

A gold cathode was evaporated either on the smooth or rough surface of the micro-porous filter. Deposition was performed at several current densities, typically at a current density of 1 mA/cm^2. In some cases, two different current densities were used. For configuration A (Fig. 2), the area was assumed to be the gross area of the surface of the filter whereas in case B (Fig. 2) the area was taken as the nominal pore cross section. Depositions were typically carried out under galvanostatic control with only the cathode (working electrode) and copper anode (counter electrode) connected to a PAR Model 273 Potentiostat/Galvanostat. In some cases the depositions were performed under potentiostatic control or control with a cyclic potential. In these cases, a third reference electrode was required.

Filter Membranes

The Poretics® filter membrane with the following specifications were used as samples representative of fine microstructures to develop the electro-deposition methods, in preparation for future samples of photonic crystals. The samples used included:

- Poretics® polycarbonate or polyester

- Track etch (PCTE) membrane filters
- 10 μm or 1μm pores and 10 μm nominal thickness

The membranes were pretreated by evaporation of Au, or carbon, or used as received and was placed in a gasket cell (see Fig. 3).

2.3 Electro-deposition Results

Many experimental depositions were carried out during the course of the program, followed by characterization steps. Table 1 in Appendix A summarizes the key experiments performed in the course of the investigation. After electrochemical deposition, light optical microscopy and scanning electron microscopy applied to the resulting filter membranes allowed a description of the general morphology of the deposit. The categories in the schematic in Fig. 4 classify the degrees of filling or partial filling that occurred and provides a key for some of the descriptions of the resulting deposit found in Table 1.

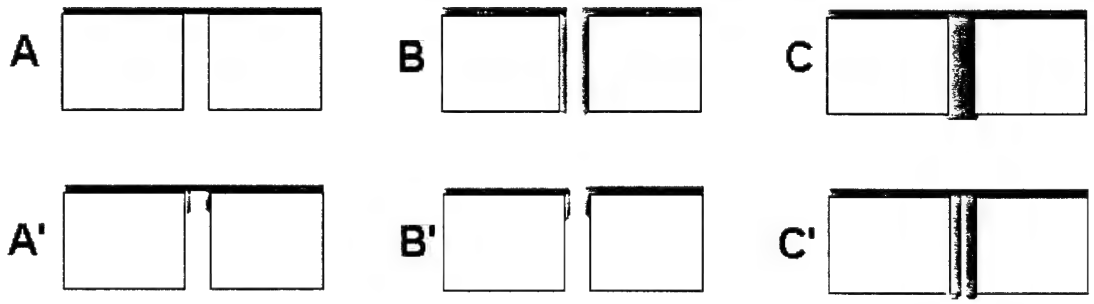

Fig. 4. Schematic illustrating the morphologies observed in the electrochemical backfilling experiments.

The deposit tended to nucleate along the walls of the pores and then grow inward. Typically, successful deposition of Cu in the pores occurred only when there was very good contact between the filter and the backing electrode. Good contact was attained for the filter on a smooth Au/Ti/Si surface. The best contact was obtained by evaporating a Au cathode directly on the porous material.

2.3.1 Electrodeposition in Acid Copper

For configuration B in Fig. 2., the acid copper electrolyte began to fill the 10 μm porous membrane only after a sufficiently long time of deposition and at a sufficiently high current

density of 5 mA/cm^2 of pore area (see Table 1). The nucleation of Cu begins along the walls of the pores, as shown in Fig. 5, appearing to grow spirally. Complete pore filling was obtained from the acid copper electrolyte in membranes with 1 μm pore dimension under conditions of cyclic potential control as shown by the cross-section in Fig. 6. The currents that flow during the cyclic potential appear in Fig. 7. As shown in Fig. 7, the cycle passed a small quantity of anodic (positive) current as indicated by the positive currents at the beginning and end of the cycle. For the 1 um porous membrane plated using configuration A (see Fig. 2), the Cu did not begin to nucleate down the pore when the Au nucleation layer faced the electrolyte with a relatively high current density and a long time for electrodeposition.

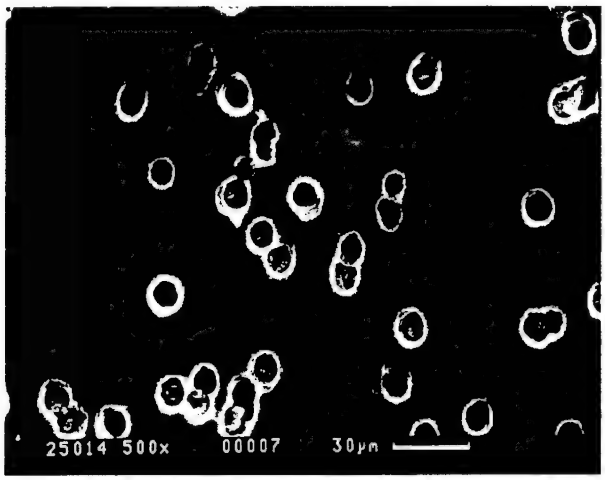

Fig. 5. Acid copper deposition into membrane with 10 um pores. The deposition proceeded at 5 mA/cm2 of pore area using configuration B shown in Fig. 2.

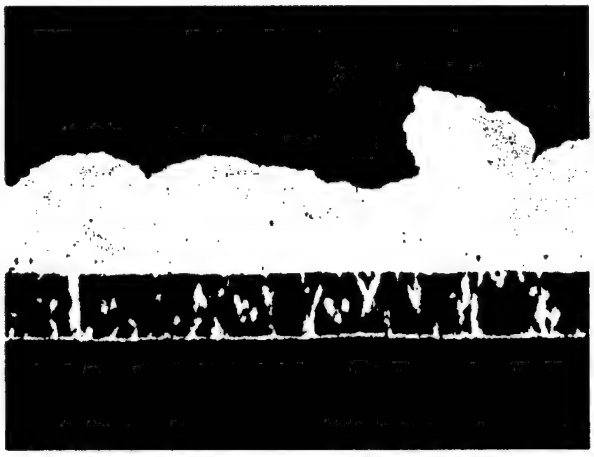

Fig. 6. Cross section showing the Cu deposit from a cyclic deposition (50 mV/s scan as shown in Fig. 7) in a 1 μm porous membrane from acid copper. Configuration of the electrochemical cell is that shown in Fig. 2B.

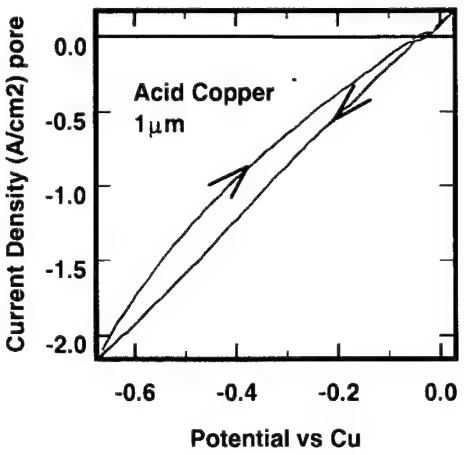

Fig. 7. Current versus voltage for the cyclic deposition of Cu from an acid copper bath.

2.3.2 Electrodeposition in Copper Pyrophosphate

A. No Additive

In the absence of the additive typically used as a 'leveling agent', Cu pyrophosphate produced deposits in the porous filters. Preliminary experiments using the Cu pyrophosphate bath involved first soaking the filter in butanol before flattening it to a smooth Au plated substrate. Deposition of Cu at 1 mA/cm^2 pore over 7 hours produced a growth of copper through the filter as shown by the micrographs in Figs. 8 – 10. The filter was peeled from the Au substrate. Some pores were not completely filled. From these pores, it appears that the copper grows by nucleation at the pore walls (Fig. 10) and grows in a screw-like fashion. This growth tends to leave a void in the center of the resulting columns of copper. Some pores showed no Cu since they were not continuous to the substrate (Fig. 11). The filter was dissolved in methylene chloride, the resulting mixture filtered. The Cu deposited in the pores was thus collected. Figure 12 shows the mushroom-shaped copper particles collected.

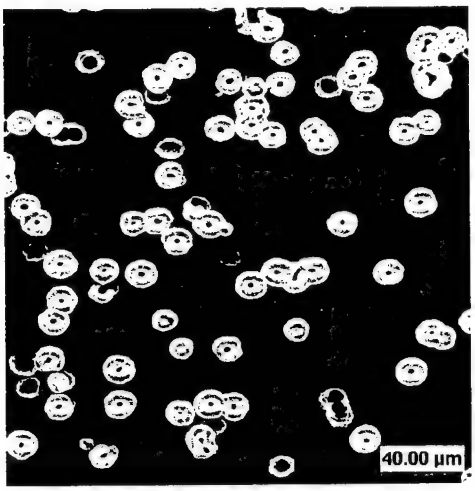

Fig. 8. Deposition in 10 µm filter at a current density of 1 mA/cm^2 pore for 7 hours using configuration in Fig. 2 B.

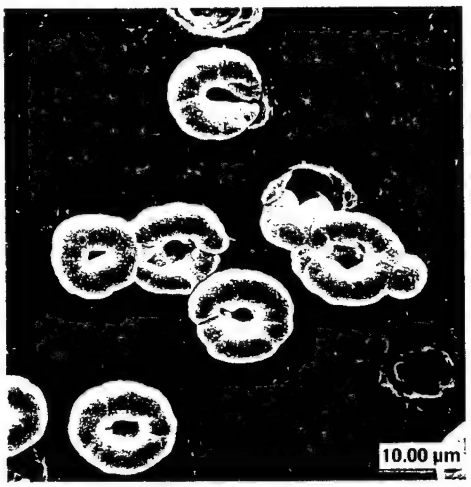

Fig. 9. Higher magnification of the deposition of Fig. 8.

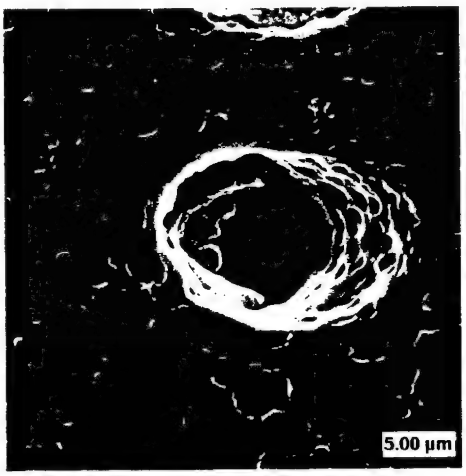

Fig. 10. Nucleation of deposition under conditions described for sample in Fig. 9.

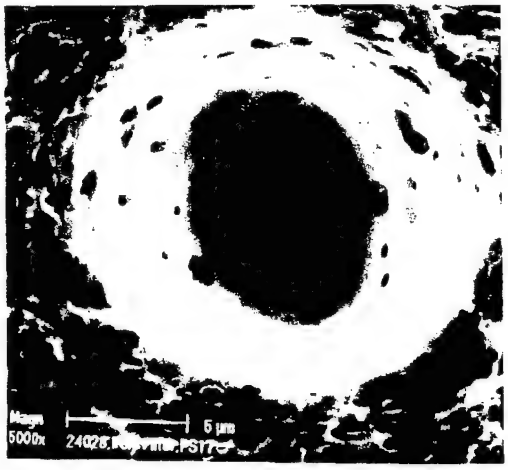

Fig. 11. Pore that did not penetrate entire membrane

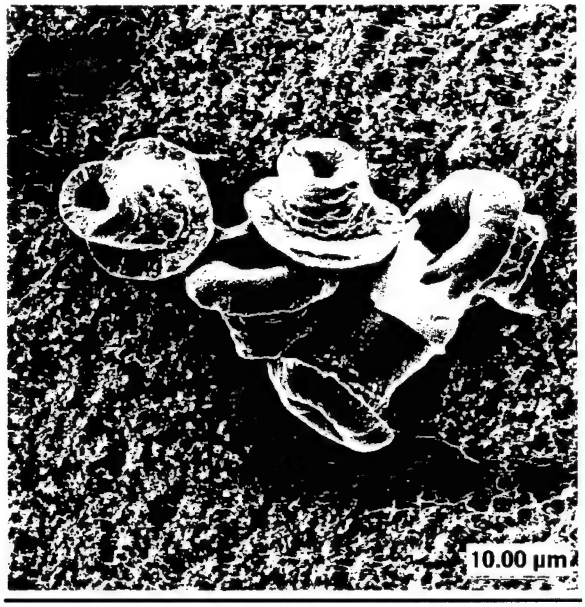

Fig. 12. Micrograph showing deposit after dissolving the membrane.

B. Additive and Elevated Temperature

As an attempt to improve uniformity of the growth of the Cu in the pore, to have it grow uniformly throughout the pore and not just along the wall, experiments were performed at elevated temperature in conjunction with the additive, of 2,5-dimercapto-1,3,4-thiadiazole. These conditions lead to a more level or bright deposit. Both of the configurations represented in Fig. 2 were considered. The results appear in Table 1. Although complete filling of the 1 μm pores was accomplished using configuration B of Fig. 2, with a 1mA/cm^2 pore current density for 5 hour deposition, these same chemical and physical conditions did not allow for sufficient filling of the 10 μm pore. Regardless of the current density, plating time or configuration, the 10 μm pores were not filled using the 'leveling' conditions. The best result that could be achieved was some coating of the walls of the pores (condition B or B' in Fig. 4).

One of the steps considered desirable in the overall process outline by the schematic in Fig. 1 is a first formation of a structural layer with nucleated pores followed by complete filling. This was accomplished for the 1 μm porous filter using the Cu pyrophosphate bath with the leveling agent at room temperature. A gold cathode was deposited on the rough side of a 1 μm porous polycarbonate membrane filter. The plating condition was that shown in Fig. 2 A such that the glossy side that did not have the gold cathode faced the insulating glass during an initial

deposition. The deposition was performed at a current density of 1 mA/cm^2 for 7 hours followed by a current density of 5 mA/cm^2 for a much shorter time. The deposition did not extend into the glass/filter interface as shown in Fig. 13, but only penetrated incompletely into the pores. It was then possible to turn the filter over and continue the deposition into the pores for complete filling as shown in Fig. 14.

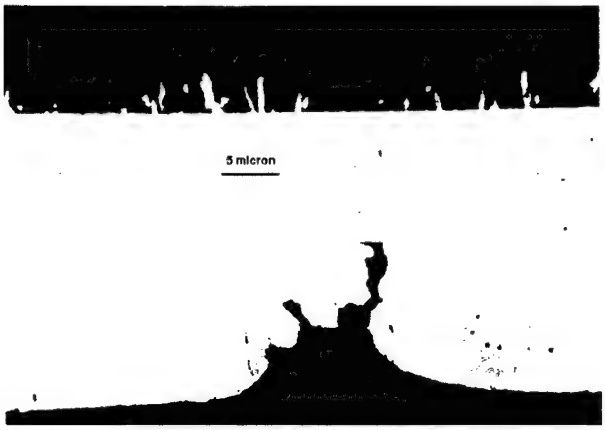

Fig. 13. Cross section showing the deposit as formed at a current density of 1 mA/cm2 for 7 hours followed by a current density of 5 mA/cm^2 for between 1-2 hours. The cell configuration is that shown in Fig. 2A. The electrolyte is Cu pyrophosphate with the leveler. Electrodeposition was performed at room temperature.

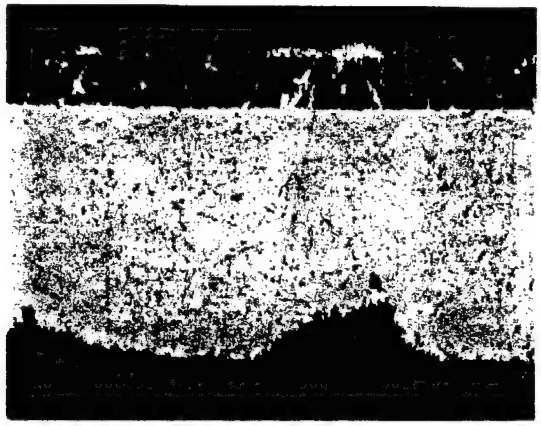

Fig. 14 Complete filling of the sample from Fig. 13 after turning over the membrane for plating on the reverse side.

C. Voltage Sweep Plating Compared to DC

Although constant current electrodeposition filled 1 μm pores as shown by the cross section, deposition in the larger 10 μm structures resulted in the formation of hollow tubes, as shown in Fig. 15.

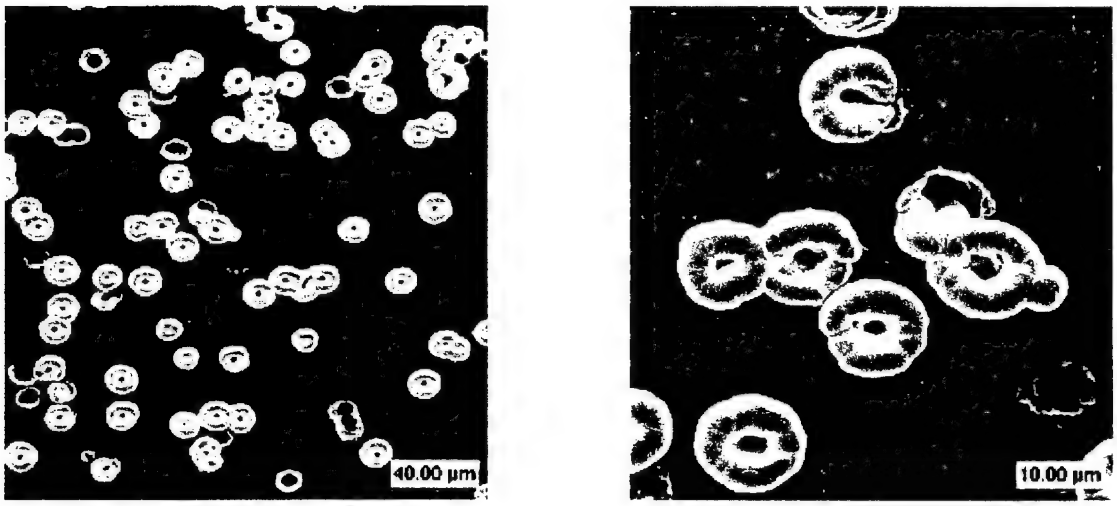

Fig. 15. Copper deposits extending through Poeretics filter with 10 µm pores, shown at two magnifications. Note that the nucleation occurred at the walls of the pores, leaving a hollow center.

Application of a sawtooth potential between the cathode and the copper counter elecrode produced more uniform filling of the pores from both the acid Cu and Cu pyrophosphate baths. Figure 16 shows the typical current vs voltage response for the cyclically applied potential deposition from a copper pyrophosphate electrolyte.

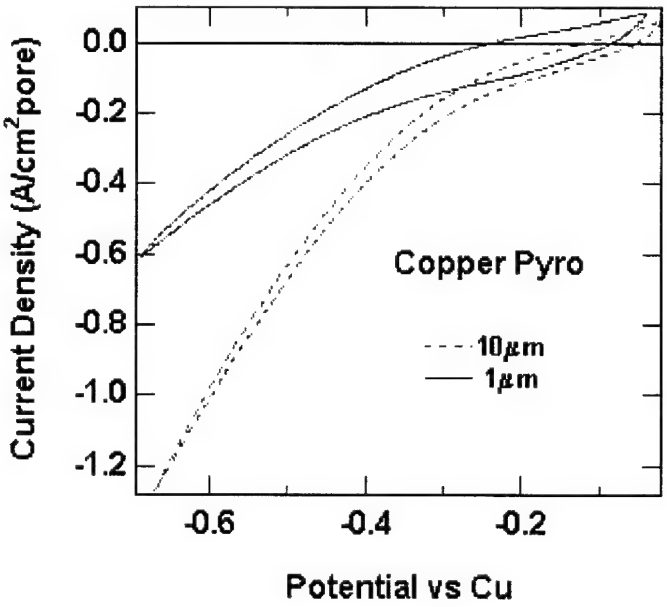

Fig. 16. Typical current vs. voltage response for an applied voltage cycle to the gold cathode base of the porous material in a copper pyrophosphate electrolyte. The current is normalized to the manufacturer's pore cross-sectional area specification.

Experiments were performed in which micro-porous filters were back-filled with Cu via an electrochemical deposition process using a cyclically applied potential using configuration B of Fig. 2 and compared to corresponding direct current or potential methods. Figure 17 shows the remaining stalks of metallization from cyclic electrodeposition in the 10 μm filter. Dissolution by methylene chloride removed the polymeric material of the filter left the remaining Cu "stalk-like" structures. For the experiment giving the structures in Fig. 17, the net quantity of cathodic charge passed was 63 coulombs. As can be seen the cyclic deposition provides good back-filling.

In contrast to the results from the cyclic experiments, Fig. 18 shows the remaining electrodeposited Cu after dissolution of the filter that was prepared at a constantly applied voltage of –0.7 V versus Cu with a total charge of 195.8 coulombs. The quantity of charge for the sample of Fig. 18 exceeds the net cathodic charge for the cyclic deposition of Fig. 17. However, the resulting deposit, as shown in Fig. 18, is considerably less dense yielding hollow tubes (compare Fig. 18 to Fig. 17). These results show the superior performance of an oscillatory electro-deposition method for efficiently backfilling microporous structures.

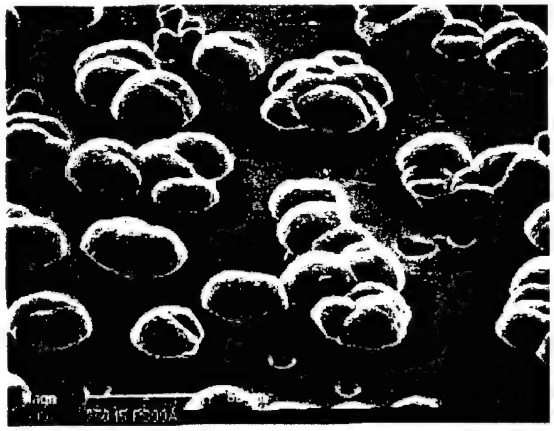

Fig. 17. Remaining structure after dissolution of the 10 μm porous polymeric filter. The Cu "mushrooms" were electro-chemically deposited by cyclic potentiodynamic deposition from a copper pyrophosphate bath. The cyclic voltage was scanned at a rate of 500 mV/s.

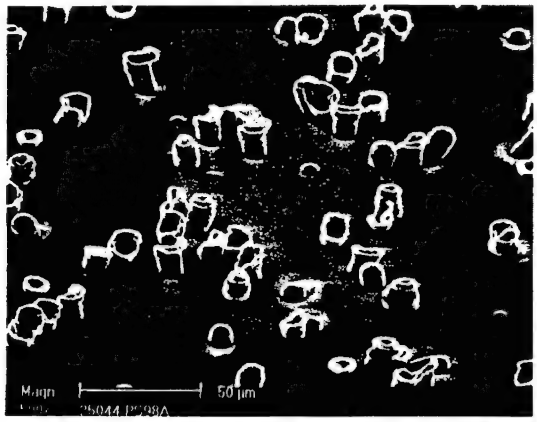

Fig. 18. Remaining structure after dissolution of the 10 μm porous polymeric filter. The Cu "cyclinders" were electrochemically deposited by cyclic potentiostatic deposition from a copper pyrophosphate bath at -0.7 V versus Cu.

2.3.3 Two Dimensional Model Substrate

We have considered experiments to determine the extent that electro-deposition can grow structures perpendicular to the plane of the substrate. A test device was constructed that allowed direct microscopic observation of the nucleation of electrocrystallized metal in complex structures as a function of variations in the plating process parameters. The motivation of this experiment was to enable a direct observation of how different plating process parameters influence the deposition in such structures

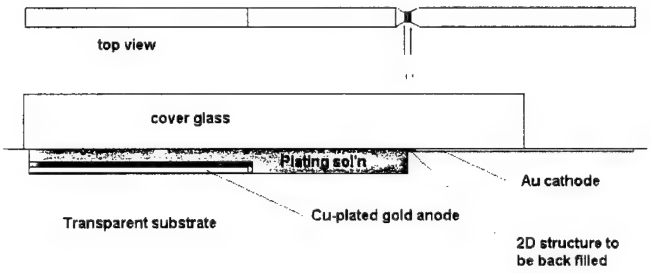

Fig. 19. Schematic of the electrochemical back-filling test device. The device allows deposition of metal (Cu) in a complex 2D structure with real-time microscopic viewing.

Fig. 20. Micrograph (left photo) of the 2D structure between the electrolyte trough and the gold cathode (mark = 100 mm), and detail (right photo) of the 2D structure (mark = 20 mm).

Deposition onto the Two Dimensional Model Substrate

The structure described in Figs. 19 and 20 includes a gold cathode connected via an etched pattern of channels to a trough and Cu-plated gold anode in the plane of a glass surface. A drop of plating solution may be placed on the surface and then covered with a glass cover slide. The application of a negative current to the gold cathode caused Cu to deposit into the planar patterned surface. The electro-crystallizing Cu nucleates at the channels of the pattern at the

cathode (Fig. 21), but as the deposition proceeds, Cu dendrites grow in all directions even pushing perpendicular to the planar surface (Fig. 22). The structure does not contain the electrodeposit. Even after loading the cover slide to >7kdyne/cm^2, the Cu dendrites squeezed out of the channels and between the cover-slide and substrate, and protruded in the direction perpendicular to the plane.

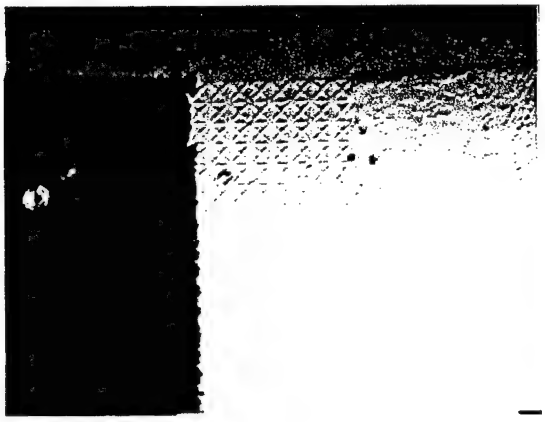

Fig. 21. Deposition across the 2D structure at 106 seconds, shortly after application of the current.

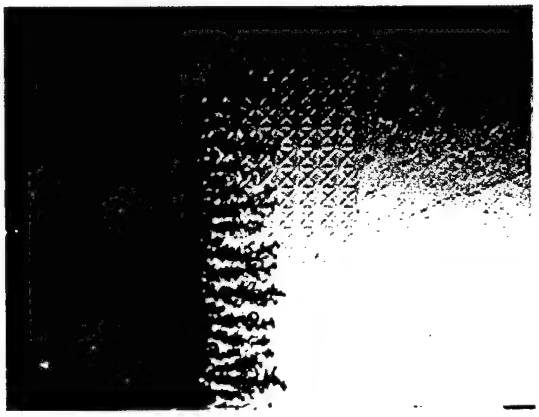

Fig. 22. Electro-deposit after 1550 seconds of deposition.

Diffusion across the structure, covered by the cover glass, occurred rapidly and completely as evidenced by results from the following experiment. The structure was covered with water and a cover glass to leave the channels filled with water. The cover glass was loaded with > 7 kdyne/cm^2. A dye was introduced on the side opposite the cathode. The layer of dye was so thin that it could not be visually detected in the solution. However, as the dye penetrated by diffusion across the structure, it adsorbed on the surface to give a visual indication of its transport. This occurred within 30 minutes of introducing the dye.

2.4 Electrodeposition Summary

This work demonstrates the general robustness of electrochemical back filling of micro-porous membranes. Electro-deposited Cu from acid copper baths and copper pyrophosphate baths tend to nucleate from an evaporated Au cathode base along the walls of the porous structure. While this poses no problems for electrodeposition in 1 μm structures, direct current electrodeposition in larger structures results in the formation of hollow structures. However, the

tendency for the deposition of hollow structures in the larger pores (10 μm versus 1 μm) can be overcome, at least in the case of acid copper and copper pyrophosphate, through deposition under conditions of controlled applied cyclic potential. Others have used similar approaches for the electrodeposition of Au and Pt in micro-porous structures [3-21]. The use of cyclic polarization of the cathode appears to be a key to the uniform backfilling of micro-porous structures by electrodeposition.

The robustness of the electrochemical method for back filling micro-porous structures has been illustrated by attempts to view the deposition on a two dimensional model structure. The deposition nucleates along the microstructure, but the deposition was very difficult to contain within the two dimensional structure since the dendridic growth of the deposit pushed away from the two dimensions.

3.0 Metallized Micro-structures by Self-assembly

An alternative method of preparing metallized microstructures was examined late in the program, with relatively interesting results. The method involved self-organization or self-assembly, promoted by using polymer micro-spheres, and a process developed at RSC.

Self-assembly and sol-gel techniques were used by Drs. Young Chung and Les Warren at RSC to prepare high index oxide-based microstructures. These materials can be useful as photonic crystals from the visible range to about 5 or 6 μm IR, depending on the specific compositions used. A sol-gel method was used, which permits the formation of glasses and ceramics by a chemical hydrolysis reaction in liquid solution at room temperature. The resulting gel can be dried and heat-treated at elevated temperature to form various types of solids, including fine powders, micro-spheres, thin films, and micro-porous bodies. There are issues with shrinkage and cracking that may need to be mitigated. A recent development in Organically Modified Silicates (ORMOSILs) utilizes similar chemistry, but provides less brittle materials. Accurate control of the microstructure involves many interdependent variables. Our initial efforts tried silica and high index oxides (e.g., titania) to provide self-assembled periodic micro-porous structures of dimensions appropriate for future photonic crystals in the infrared, and 2D and 3D photonic lattice parameters which can be tailored to the designs. Metallization of these structures was also carried out. Both the dielectric materials and metallized microstructures showed significant promise, and it is believed that the methods tried here will prove valuable for photonic crystals over a wide range of lattice parameters.

3.1 Self-assembly Process

Our preliminary studies showed that it is difficult to make thick 3-D close packed structures of any reasonable size by self-organization. "Crystals" that form through sedimentation of hard sphere colloidal dispersions have random stacking of the close packed planes perpendicular to the settling force (gravitational or centrifugal). However, we believe that when a colloidal "crystal" is grown on a substrate with a template hole pattern commensurate with the (100) plane of a face centered cubic crystal, a pure *fcc* PBG crystal can form. In this fashion, the (100) face of the substrate induces a 3-D *fcc* structure due to the fact that there is

only one possible way the second layer can be placed on the holes created by the first layer. A micrograph of a monolayer portion of self-assembled polymer spheres on glass is shown in Fig. 23 below.

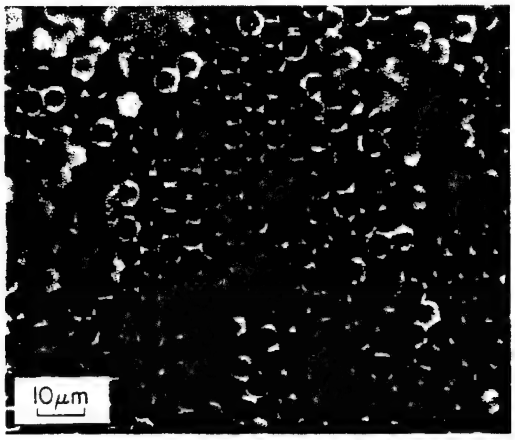

Fig. 23. Self-assembled polymer spheres.

3.2 Self-assembly Process for Dielectric Microstructures

Incorporating a sol-gel process in the sedimentation growth of microstructures is an effective means to make a low temperature oxide matrix around the spheres without destroying the ordered structure. Since it is a solution process, the matrix can conform to any scale and shape. A simple self-assembly technique for generating closely packed arrangements of polystryrene spheres as templates for sol-gel oxide photonic crystal-like structures was tried. The procedure involved centrifugal settling of appropriate size uniform spheres from a sol solution onto a substrate template dimpled with a square array pattern, the spacing being calculated for a specific PBG frequency. Subsequent solvent evaporation, drying, and heating high enough to burn out the polymer spheres resulted in an air sphere/oxide matrix structure. A micrograph of a silica encapsulated air sphere monolayer (on a non-patterned glass substrate) is shown in Fig. 24.

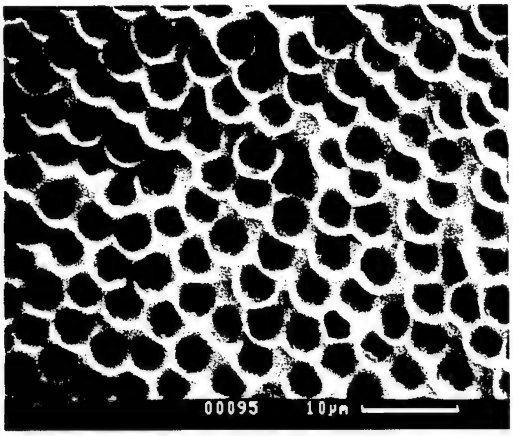

Fig. 24. Air spheres in silica matrix.

The material surrounding the polymer microspheres has porosity on the order of nanometer sizes. Slow heating at high temperature allows the polymer to slowly burn off, leaving the silica or titania structures around air spheres of about the same dimensions as the polymer microspheres. The length of time needed for a complete burn-off is best established by experiments. A cross section of the structure is shown in Fig. 25, in which the polymer spheres are seen to be not quite completely burned out in that experiment.

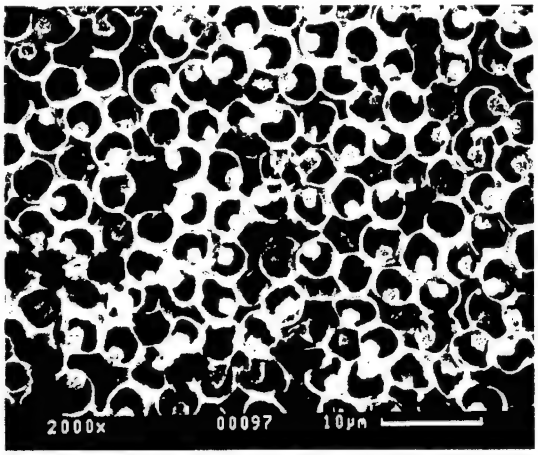

Fig. 25. Air sphere/silica matrix cross section.

3.3 Fabrication Sequence for Porous Oxide Microstructures

The steps below are the 'recipe' for development of dielectric and/or metallic microstructure for photonic crystal applications such as high reflectivity (low emissivity) materials:

Step 1: Prepare a simple cubic micro-structured template on a flat substrate, such as a silicon wafer, with a square array of etched holes or dimples made by standard photo-lithographic techniques. The depth and radius of these holes are designed to be slightly larger than the radius of the polymer micro-spheres, which will reside in the holes. This template is enclosed with walls so that thick 3-D ordered structures can be grown. This step is believed to be the key to making regular microstructures that can exhibit photonic crystal behavior. (This step was tried enough to convince us that the method will work, but not fully implemented at this time, due to limited resources. We believe the process will work, and have seen enough evidence to want to pursue the method in the future.)

Step 2: Prepare a suspension of appropriate sized polymer micro-spheres in a titania (or other oxide) sol. A "sol" is a colloidal suspension of solid particles formed by the hydrolysis reaction of a metal alkoxide dissolved in the liquid.

Step 3: Fill the template container with the above suspension. The ordered 3-D microstructure can be obtained by slow gravitational sedimentation of the polymer spheres in the sol without convection. Filling of the holes/dimples on the template with the polymer spheres forms the first ordered layer. The second non-random layer will form on the holes of the first layer, and so forth. This layer by layer growth will form a highly ordered thick 3-D polymer sphere structure.

Step 4: Carefully remove excess solution from the template container after completion of sphere sedimentation. Gelation of the silica or titania sol by further reaction with atmospheric water and condensation during evaporation of the remaining solvent results in a rigid composite of polymer spheres within a silica or titania gel.

Step 5: Heat the composite slowly at 500°C, whereby the polymer spheres are burned off, leaving behind ordered air spheres in the titania matrix. Heating at higher temperatures can densify this resulting structure further, albeit with some shrinkage.

Structures of this kind can be prepared with oxides other than titania, e.g., silicon, iron, or tin, using the same procedure. In addition, advanced ferroelectric structures can be fabricated using a mixture of the appropriate metal alkoxides in the sol solution; subsequent thermal

processing will result in a micro-crystalline ferroelectric photonic crystal framework which have the potential of tunability by mean of an electric field.

3.4 Self-assembly Process for Metallic Microstructures

Metallized PBG structures can also be fabricated using a modification of the above procedure. Substituting a reactive metal salt solution for the sol, followed by slow solvent evaporation and subsequent heating to 250°C will result in novel photonic crystals or photonic crystal-like structures comprising ordered polymer beads encapsulated with metal. Figure 26 illustrates such a composite structure.

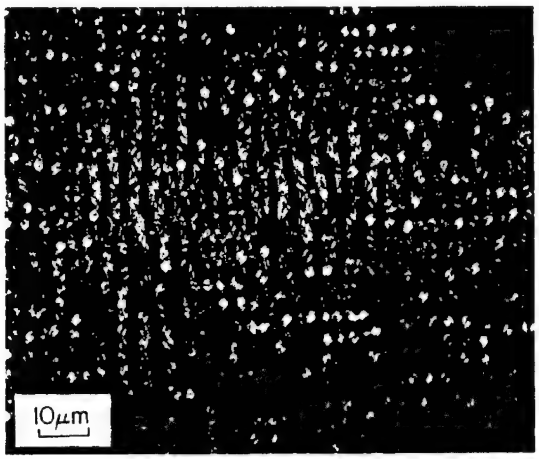

Fig. 26. Metallized polymer spheres developed by self-assembly.

Metals that we tried included palladium, gold, and copper; these can be further thickened if required by electroless metals and/or electroplating, as described earlier in this report. With certain metals, the polymer spheres can be burned out leaving air-sphere metallic structures.

3.5 Summary of Metallized Microstructures by Self-assembly

The effort described above established an alternative path for fabrication of metallized microstructures and photonic crystals by a self-assembly process. We developed a recipe for materials preparation, using polymer microspheres as guides for creating periodic structures, and demonstrated material fabrication, creating dielectric microstructures consisting of a silica or titania matrix around polymer spheres. We also demonstrated a process to pyrolize and eliminate the polymer microspheres, resulting in silica or titania matrix around air microspheres. If properly ordered, such structures are expected to exhibit photonic bandgaps. This effort also

demonstrated automatic metallization of the structures by dissociation of metal salts included in the gel that formed the matrix around the microspheres. Metals that we tried included palladium, gold, and copper. The films can be further thickened if required by electroless deposition or electrodeposition methods studied extensively in this effort.

References

References to the electrochemical approach are included in 2-21 and references to the sol-gel approach appear in 22 – 25.

1. DARPA/MTO initiative on Steered Agile Beams (STAB); numerous approaches are being investigated, including a program entitled "Photonic Bandgap Agile Beam Steering", led by RSC, in teaming with UCLA, MIT, and Boeing. The team's approach is to use the super-prism properties of dielectric and/or metallic photonic crystal for beam steering. The STAB programs kicked off in August, 2000.
2. C. Ogden, and D. Tench, *J. Electrochem.* Soc., 128(3), 539 (1981).
3. R. Penner and C. Martin, *Anal. Chem.* 59, 2625 (1987)
4. F. Cheng, J. Schimpf, C. Martin, *J. Electroanal. Chem.*, 284, 499 (1990).
5. K. Uosaki, K. Okazaki, H. Kita, H. Takahashi, *Anal. Chem.*, 62, 625 (1990).
6. C. Foss, G. Hornyak, J. Stockert, C. Martin, *J. Phys. Chem.*, 96, 7497 (1992).
7. C. Liu, W. Chen, C. Martin, *J. Membrane Sci.*, 65, 113 (1992).
8. C. J. Brumlik and C. Martin, *Anal. Chem.* 64, 1201 (1992).
9. C. Martin, *Science*, 266, 1961 (1994).
10. C. Brumlik, V. Menon and C. Martin, *J. Mater. Res.*, 9(5), 1174 (1994).
11. C Foss, G. Hornyak, J. Stockert and C. Martin, *J. Phys. Chem.*, 98,2963 (1994)
12. V. Menon and C. Martin, *Anal. Chem.* 1920(1995).
13. M. Nishizawa, V. Menon, C. Martin, *Science*, 268, 700 (1995).
14. C. Martin, *Chem. Mater.*, 8, 1739 (1996).
15. J. Hulteen, V. Menon and C. Martin, *J. Chem. Soc.*, Faraday Trans., 92(20), 4029 (1996)
16. V. Cepak, J. Hulteen, G. Che, K. Jirage, B. Lakshmi, E. Fisher, C. Martin, *J. Mater. Sci*, 13(11), 3070 (1998)
17. C. Martin and D.T. Mitchell, *Anal. Chem.*, 67(13), 322A (1998).
18. S. Sapp, D. Mitchell, C. Martin, *Chem. Mater.*,11, 1183(1999)
19. Forrer, F. Schlottig, H. Siegenthaler and M. Textor, *J. Appl. Electrochem.*,30, 533 (2000).
20. L. Li, *J. Mater. Sci.. Technol.*, 16(1),50 (2000)
21. D. Dobrev, J. Vetter, N. Angert, R. Neuman, Electrochium. *Acta*, 45, 3117 (2000)
22. A.V. Balaaderen, R. Ruel, and P. Wiltzius, "Template-directed Colloidal Crystallization," *Nature* **385**, 321, 23 Jan. 1997.
23. O.D. Velev, T.A. Jede, R.F. Lobo, and A.M. Lenhoff, "Porous Silica via colloidal Crystallization," *Nature* **389**, 448, 2 Oct. 1997.
24. J.E.G.J. Wijnhoven and W.L. Vos, "Preparation of Crystals Made of Air Spheres in Titania," *Science* **281**, 802, 7 Aug. 1998.
25. G. Subramania, K. Constant, R. Biswas, M.M. Sigalas, and K.M. Ho, "Optical Photonic Crystals Fabricated from Colloidal Systems," *Applied Physics Letters* **74**, 3933 (1999).

APPENDIX A.

Table of Electrodeposition Studies Summary

See explanation of the column headings at the end of the table.

Sample	Filter Type & Pore Size	Side of filter with deposit	Configuration (a)	Observations of the Cu deposit on side facing the electrolyte (b)	Observations of the Cu deposit on side facing the insulator (b)	Current Density (A/cm^2) (c)	Time (hour)	Charge (Coul.)	Comments
PS87	PC 10μm	shiny	NC/Au/PS/ACu	Little seen	none	5Po	2		
PS88	PC 10μm	shiny	NC/Au/PS/ACu	Little seen	none	1Po	6		
PS89	PC 10μm	shiny	NC/Au/PS/ACu	pores partially filled, B'	mostly Cu covered	5Po	6		
PS94	PC 1μm	shiny	NC/Au/PS/ACu	Filled, C	Cu covered		5.5	50	Cyclic pot.
PS90	PC 1μm	shiny	NC/PS/Au/ACu	Little seen		1	1		
PS91	PC 1μm	shiny	NC/PS/Au/ACu	Little seen		1	1		
PS92	PC 1μm	dull	NC/PS/Au/ACu	Little seen		1	1		
PS93	PC 1μm	shiny	NC/PS/Au/ACu	Little seen	Cu covered	1	6.7		
PS27	PC 10μm	dull	NC/Au/PS/CuP	in some pores	pores not closed, B	1Po	7		
PS28	PC 10μm	shiny	NC/Au/PS/CuP	covered	pores not closed, B	1Po	7		
PS96	PC 10μm	dull	NC/Au/PS/CuP	Donuts + mushrooms, C	Cu covered		6	50	Cyclic pot.
PS97	PC 10μm	dull	NC/Au/PS/CuP	Pores full, mushrooms, C	Cu covered		7	100	Cyclic pot
PS98	PC 10μm	shiny	NC/Au/PS/CuP	Pores full, donuts, C	Cu covered		5	500	Cyclic pot
PS99	PC 10μm	dull	NC/Au/PS/CuP	Pores full, mushrooms, C	Cu covered		4		-0.7 V applied
PS95	PC 1μm	dull	NC/Au/PS/CuP	Some pores filled	Cu covered w/pores		5	50	Cyclic pot.
PS29	PC 10μm	dull	NC/PS/Au/CuP	covered	Cu donuts,full	1	6.3		
PS30	PC 10μm	shiny	NC/PS/Au/CuP	covered	Cu donuts	1	6.3		
PS31	PC 10μm	shiny	NC/PS/Au/CuP	covered	Cu donuts	1,10	20,6		
PS32	PC 10μm	dull	NC/PS/Au/CuP	covered	pores filled	1,10	20,6		
PS33	PC 10μm	shiny	NC/PS/Au/CuP	covered	few spots, 5%	1,10	6,2		
PS34	PC 10μm	dull	NC/PS/Au/CuP	covered	none	1,10	6,2		
PS39	PC 1μm	shiny	NC/PS/Au/CuP	covered	2 spots 10%	1,5	6,1 to 2		
PS44	PC 1μm	dull	NC/Au/PS/CuPLT	a little Cu	most pores full	1 Po	5		

Sample	Filter Type & Pore Size	Side of filter with deposit	Configuration (a)	Observations of the Cu deposit on side facing the electrolyte (b)	Observations of the Cu deposit on side facing the insulator (b)	Current Density (A/cm^2) (c)	Time (hour)	Charge (Coul.)	Comments
PS45	PC 1μm	shiny	NC/Au/PS/CuPLT	a little Cu	most pores full	1 Po	5		
PS46	PC 1μm	dull	NC/Au/PS/CuPLT	a little Cu	covered	10 Po	1		
PS47	PC 1μm	shiny	NC/Au/PS/CuPLT	a little Cu	covered	10 Po	1		
PS50	PC 1μm	dull	NC/Au/PS/CuPLT	B, 10% of area	B	10 Po	0.5		
PS51	PC 1μm	shiny	NC/Au/PS/CuPLT	B, 10% of area	B	10 Po	0.5		
PS52	PC 1μm	dull	NC/Au/PS/CuPLT	B, 10% of area	B	3 Po	3.3		
PS53	PC 1μm	shiny	NC/Au/PS/CuPLT	none	B	3 Po	3.3		
PS54	PC 1μm	dull	NC/Au/PS/CuPLT	none	B	30Po	0.3		
PS55	PC 1μm	shiny	NC/Au/PS/CuPLT	none	B	30Po	0.3		
PS58	PC 10μm	dull	NC/Au/PS/CuPLT	B	B, detached	1 Po	5		
PS59	PC 10μm	shiny	NC/Au/PS/CuPLT	C,B,B'	B, detached	1 Po	5		
PS60	PC 10μm	dull	NC/Au/PS/CuPLT	None	B, detached	3 Po	3.3		
PS61	PC 10μm	shiny	NC/Au/PS/CuPLT	None	B, detached	3 Po	3.3		
PS62	PC 10μm	dull	NC/Au/PS/CuPLT	B,B' v. thin	B	5Po	1		
PS63	PC 10μm	shiny	NC/Au/PS/CuPLT	B,B' med.	B	5Po	1		
PS64	PC 10μm	dull	NC/Au/PS/CuPLT	B,B' thin	B	5Po	0.5		
PS65	PC 10μm	shiny	NC/Au/PS/CuPLT	None	B, detached	5Po	0.5		
PS67	PC 10μm	shiny	NC/Au/PS/CuPLT	C, B, A, A'	B, detached	5Po	0.5		
PS68	PC 10μm	dull	NC/Au/PS/CuPLT	B,B' med	B, detached	15Po	0.33		
PS69	PC 10μm	shiny	NC/Au/PS/CuPLT	C,B'	B, detached	15Po	0.33		
PS74	PC 1μm	dull	NC/Au/PS/CuPLT	None	A	10Po	1.5		
PS75	PC 1μm	shiny	NC/Au/PS/CuPLT	None	A	10Po	1.5		
PS76	PC 1μm	dull	NC/Au/PS/CuPLT	None	A	1Po	15		
PS78	PC 1μm	dull	NC/Au/PS/CuPLT	None	A	1Po	15		
PS79	PC 1μm	shiny	NC/Au/PS/CuPLT	None	A	1Po	15		
PS80	PC 1μm	dull	NC/Au/PS/CuPLT	None	A on part of surface	10,1Po	6.5		

Sample	Filter Type & Pore Size	Side of filter with deposit	Configuration (a)	Observations of the Cu deposit on side facing the electrolyte (b)	Observations of the Cu deposit on side facing the insulator (b)	Current Density (A/cm^2) (c)	Time (hour)	Charge (Coul.)	Comments
PS81	PC 1μm	shiny	NC/Au/PS/CuPLT	None	A on part of surface	10,1Po	6.5		
PS82	PC 10μm	shiny	NC/Au/PS/CuPLT	None	A	5Po	20		
PS83	PC 10μm	shiny	NC/Au/PS/CuPLT	None	B	5Po	6		
PS84	PC 10μm	shiny	NC/Au/PS/CuPLT	None	B'	5Po	2		
PS35	PC 1μm	shiny	NC/PS/Au/CuPL	covered	covered	1,5	7,1 to 2		
PS36	PC 1μm	dull	NC/PS/Au/CuPL	covered	none	1,5	7,1 to 2		
PS37	PC 1μm	shiny	NC/PS/Au/CuPL	covered	none	1,5	6,1 to 2		
PS42	PC 1μm	shiny	NC/PS/Au/CuPLT	covered	most pores full	1	5		
PS43	PC 1μm	dull	NC/PS/Au/CuPLT	covered	most pores full	1	5		
PS48	PC 1μm	dull	NC/PS/Au/CuPLT	a little Cu	covered	1	1		
PS49	PC 1μm	shiny	NC/PS/Au/CuPLT	A	B, 20%	1	1		
PS56	PC 10μm	dull	NC/PS/Au/CuPLT	B,B' thick	B	1	1		
PS57	PC 10μm	shiny	NC/PS/Au/CuPLT	B, detached	A',B,B'	1	1		
PS66	PC 10μm	dull	NC/PS/Au/CuPLT	B, detached	B	1	1		
PS70	PC 10μm	dull	NC/PS/Au/CuPLT	B, det.	B,B'	1	1		
PS71	PC 10μm	shiny	NC/PS/Au/CuPLT	B, det.	B,B'	1	1		
PS72	PC 10μm	dull	NC/PS/Au/CuPLT	B	B	1	0.5		
PS73	PC 10μm	shiny	NC/PS/Au/CuPLT	B	detached	1	0.5		

(a) See Fig. 2 for meaning of configuration notation

(b) Refer to Fig. 4 for meaning of the notes A,A',B,B',C,C'

(c) Po indicates that the current density in A/cm^2 is referenced to the manufacturer-specified pore cross section in which case the current density is the observed current divided by the manufacturer-specified pore cross section. Otherwise the current density is determined by dividing the observed current by the superficial surface area of the filter. No entry in this column means that the electrodeposition was carried out under potential control as described in the 'Comments' column. Two numbers separated by commas indicate that two different current levels were used in the experiment.